

Supporting Information

CO₂ superabsorption in a paddlewheel-type Ru dimer chain compound: Gate-open performance dependent on inter-chain interactions

Wataru Kosaka,^a Kayo Yamagishi,^a Hiroki Yoshida,^b Ryotaro Matsuda,^{c,e,g} Susumu Kitagawa,^{c,d,e,g}
Masaki Takata,^{f,g} and Hitoshi Miyasaka^{*a}

^a *Department of Chemistry, Division of Material Sciences, Graduate School of Natural Science and Technology, Kanazawa University, Kakuma-machi, Kanazawa 920-1192, Japan*

^b *Department of Chemistry, Graduate School of Science, Tohoku University, 6-3 Aramaki-Aza-Aoba, Aoba-ku, Sendai 980-8578, Japan*

^c *ERATO Kitagawa Integrated Pores Project, Japan Science and Technology Agency (JST), Kyoto Research Park Bldg #3-405, Shimogyo-ku, Kyoto 600-8815, Japan*

^d *Department of Synthetic Chemistry and Biological Chemistry, Graduate School of Engineering, Kyoto University, Katsura, Nishikyo-ku, Kyoto 615-8510, Japan*

^e *Institute for Integrated Cell-Materials Science (iCeMS), Kyoto University, Katsura, Nishikyo-ku, Kyoto 615-8510, Japan*

^f *Japan Synchrotron Radiation Research Institute/Spring-8, Sayo-gun, Hyogo 679-5198, Japan*

^g *RIKEN Spring-8 Center, Sayo-gun, Hyogo 679-5198, Japan*

Corresponding author*

Hitoshi Miyasaka

Department of Chemistry, Division of Material Sciences, Graduate School of Natural Science and Technology, Kanazawa University, Kakuma-machi, Kanazawa 920-1192, Japan

E-mail: miyasaka@se.kanazawa-u.ac.jp

Tel: +81-76-264-5697

Fax: +81-76-264-5742

Experimental Section

Syntheses and general procedures

All chemicals used were of reagent grade quality. All reactions and procedures were carried out under a N₂ atmosphere. PhNO₂ (= nitrobenzene) was dried by refluxing over sodium hydride, and distilled under N₂ before use. [Ru₂(*p*-F-PhCO₂)₄(THF)₂] was synthesized by following the literature methods.¹ [Rh₂(*p*-F-PhCO₂)₄(THF)₂] was synthesized in a similar manner reported previously.²

Synthesis of [Ru₂(*p*-F-PhCO₂)₄(phz)]·2PhNO₂ (1**).** A PhNO₂ solution (10 mL) of [Ru₂(*p*-F-PhCO₂)₄(THF)₂] (36 mg, 0.04 mmol) was separated to 2 mL portions (bottom layer) and placed in narrow diameter glass tubes (ϕ : 8 mm). After adding 1 mL of PhNO₂ onto the bottom layer, a PhNO₂ solution (10 mL) of phenazine (29 mg, 0.16 mmol) was carefully placed in 2 mL portions into the middle layer. These tubes were left undisturbed for a week under anaerobic condition to yield brown block crystals of **1** (25 mg, yield 53%). Elemental analysis (%) calcd for C₅₂H₃₄F₄N₄O₁₂Ru₂: C 52.71, H 2.89, N 4.73. Found: C 52.87, H 3.03, N 4.75. IR (KBr): ν (CO₂), 1554, 1412 cm⁻¹.

Synthesis of [Ru₂(*p*-F-PhCO₂)₄(phz)] (1'**).** Crystal samples of **1** were heated at 400 K under vacuum for 5 h. Elemental analysis (%) calcd for C₄₀H₂₄F₄N₂O₈Ru₂: C 51.18, H 2.58, N 2.98. Found: C 51.02, H 2.84, N 3.14. IR (KBr): ν (CO₂), 1547, 1410 cm⁻¹.

Synthesis of [Rh₂(*p*-F-PhCO₂)₄(phz)]·2PhNO₂ (2**).** Compound **2** was prepared by a similar method to that for **1**, but using [Rh₂(*p*-F-PhCO₂)₄(THF)₂] (36 mg, 0.04 mmol) instead of [Ru₂(*p*-F-PhCO₂)₄(THF)₂], yielding 30 mg of **2** (yield 64%). Elemental analysis (%) calcd for C₅₂H₃₄F₄N₂O₁₂Rh₂: C 52.54, H 2.88, N 4.71. Found: C 52.20, H 3.00, N 4.91. IR (KBr): ν (CO₂), 1573, 1405 cm⁻¹.

Preparation of [Rh₂(*p*-F-PhCO₂)₄(phz)] (2'**).** Dried compound **2'** was prepared by the same procedure used for **1'**. Elemental analysis (%) calcd for C₄₀H₂₄F₄N₂O₈Rh₂: C 50.98, H 2.57, N 2.97. Found: C 50.98, H 2.70, N 3.13. IR (KBr): ν (CO₂), 1571, 1407 cm⁻¹.

Physical measurements

Infrared (IR) spectra were measured on a KBr pellet using a Jasco FT-IR 620 spectrometer. Thermogravimetric analyses (TGA) were recorded at a Shimadzu DTG-60H apparatus under a N₂ atmosphere in the temperature range from 298 K to 573 K at a heating rate of 5 K min⁻¹. Powder X-ray diffraction (PXRD) was collected on a Rigaku RINT-2500HK diffractometer with Cu K α radiation (λ = 1.5418 Å) at room temperature. Magnetic susceptibility measurements were performed using a Quantum Design SQUID magnetometer MPMS-XL on a polycrystalline sample in the temperature range 1.8–300 K at a dc field of 1 kOe. Diamagnetic contributions were collected for the sample holder, Nujol, and for the sample using Pascal's constants.³

X-Ray crystallographic analysis for **1** and **2**

Crystal data for **1** were collected at 93 K on a CCD diffractometer (Rigaku Saturn724+Varimax) with multi-layer mirror monochromated Mo K α radiation (λ = 0.71070 Å). Crystal data for **2** were collected at 123 K on a CCD diffractometer (Rigaku Mercury70+Varimax) with graphite monochromated Mo K α radiation (λ = 0.71070 Å). A single crystal was mounted on a thin-glass loop and cooled in an N₂ gas stream. The structures were solved using direct methods (SIR2008⁴ and SHELX97⁵ for **1** and **2**, respectively), which were expanded using Fourier techniques and refined by full-matrix least-squares refinements on F^2 . The non hydrogen atoms were refined anisotropically, and hydrogen atoms were refined using riding model. These data have been deposited as CIFs at the Cambridge Data Centre as supplementary publication nos. CCDC-895511

and 895509 for **1** and **2**, respectively. Copies of the data can be obtained free of charge on application to CCDC, 12 Union Road, Cambridge CB21EZ, UK (fax: (+44) 1223-336-033; email: deposit@ccdc.cam.ac.uk). Structural diagrams were prepared using VESTA software.⁶ The void volumes of crystal structures were estimated by PLATON.⁷

Structural determination for **1'** and **2'** from X-ray powder diffraction

The grinded samples of **1'** and **2'** were sealed in a silica glass capillary (0.4 mm inside diameter). The XRPD pattern with good counting statistics was measured using a synchrotron radiation XRPD experiment with the large Debye-Scherrer camera and imaging plate as detectors on the BL44B2 beam line at the Super Photon Ring (Spring-8, Hyogo, Japan). The XRPD pattern was obtained with a 0.01° step. Cell parameters were determined by DIFFRACplus TOPAS[®] v4.2 software. A Le Bail structureless profile fitting algorithm which affords refined cell parameters and ab initio structure solution from diffraction data with direct-space method was done using FOX software.⁸ The structure refinement was performed by the Rietveld method with RIETAN-FP software.⁹ The peak shape was modeled by a Split-Pearson VII function. Soft constraints about bond distances, bond angles and dihedral angles were adapted throughout the refinement. Hydrogen atoms were placed at calculated positions, and their parameters were not refined. These data have been deposited as CIFs at the Cambridge Data Centre as supplementary publication nos. CCDC-895510 and 895508 for **1'** and **2'**, respectively. Copies of the data can be obtained free of charge on application to CCDC, 12 Union Road, Cambridge CB21EZ, UK (fax: (+44) 1223-336-033; email: deposit@ccdc.cam.ac.uk).

Gas adsorption measurements

The sorption isotherm measurements for N₂ (at 77 and 120 K), O₂ (at 90 K), NO (at 121 K), CO₂ (at 195 K) gas were carried out by using an automatic volumetric adsorption apparatus (BELSORP max; BEL inc). A known weight (ca. 100 mg) of the dried sample was placed into the sample cell and then, prior to measurements, was evacuated again using the degas function of the analyzer for 5 h at 400 K. Then the change of the pressure was monitored and the degree of adsorption was determined by the decrease of the pressure at the equilibrium state.

On the oxidation state of the [Ru₂] unit in **1**

The oxidation state of [Ru₂] unit can be known from the Ru–O_{eq} length (O_{eq} = equatorial oxygen atoms), which is quite sensitive to the oxidation state of the [Ru₂] unit and to be 2.06–2.07 Å for [Ru₂^{II,II}] and 2.02–2.03 Å for [Ru₂^{II,III}]⁺.^{10,11} The average Ru–O_{eq} length of **1** is 2.065 Å, indicating an oxidation state of [Ru^{II,II}]. Note that it is the same in **1'**.

Additional description on the crystal packing of **1** and **2**

The PhNO₂ molecules as interstitial solvents are accommodated between chains of **1** by interacting with a phenyl group of [Ru₂] unit (the distance between the center of phenyl ring and N(2) of PhNO₂ is 3.60 Å, and the shortest atomic distance is O(6)_{PhNO₂}⋯C(7)_{Ph} = 3.39(1) Å) and phz (C(5)_{Ph}⋯C(18)_{phz} = 3.30(2) Å) (Fig. 1). The chains aligned along the *b* axis, which are related in an in-phase manner, make π stacks between phenyl rings of *p*-F-PhCO₂ groups in a face-to-face fashion (a distance between the least-square phenyl planes is 3.43 Å). If the PhNO₂ molecules were not taken into account, the packing form of **1** could have a solvent accessible volume of 814.0 Å³, which corresponds to 34.2 % of the total volume.

The chain packing of **2** is also very similar to that of **1** (Fig. S3); the inter-chain [Rh₂]⋯phz distance (the *b*+*c* direction) is 11.65 Å and phenyl⋯phenyl distance of π-stacked *p*-F-PhCO₂ groups along the *b* axis is 3.49 Å.

Table S1. Crystallographic data for **1** and **2**

	1	2
empirical formula	C ₅₂ H ₃₄ F ₄ N ₄ O ₁₂ Ru ₂	C ₅₂ H ₃₄ F ₄ N ₄ O ₁₂ Rh ₂
formula weight	1184.98	1188.65
Crystal Dimensions / mm ³	0.13×0.11×0.10	0.30×0.10×0.01
<i>T</i> / K	93(1)	123(1)
Crystal system	monoclinic	monoclinic
Space group	<i>P</i> 2 ₁ / <i>n</i>	<i>P</i> 2 ₁ / <i>n</i>
<i>a</i> / Å	10.064(3)	9.977(3)
<i>b</i> / Å	11.778(4)	11.801(4)
<i>c</i> / Å	20.097(6)	20.095(6)
<i>β</i> / °	91.221(5)	90.418(4)
<i>V</i> / Å ³	2381.6(13)	2365.9(12)
<i>d</i> _{calcd} / g cm ⁻³	1.652	1.668
<i>Z</i>	2	2
<i>μ</i> (Mo-Kα) / cm ⁻¹	7.20	7.82
Reflections collected	18812	21810
Unique	5424 (<i>R</i> _{int} = 0.055)	4143 (<i>R</i> _{int} = 0.081)
<i>R</i> 1 (<i>I</i> > 2.00σ(<i>I</i>)) ^a	0.0941	0.0818
<i>R</i> (all reflection) ^a	0.1201	0.1044
<i>wR</i> 2 (all reflection) ^b	0.2245	0.1645
GOF on <i>F</i> ²	1.249	1.127
CCDC no.	895511	895509

^a $R1 (R) = \sum ||F_o| - |F_c|| / \sum |F_o|$. ^b $wR2 = [\sum w(F_o^2 - F_c^2)^2 / \sum w(F_o^2)]^{1/2}$.

Table S2. Selected bond lengths (Å) angles (°) for **1** and **2** (M = Ru for **1** and Rh for **2**)

	1	2
M(1)–O(1)	2.069(6)	2.027(6)
M(1)–O(2) [*]	2.057(6)	2.038(6)
M(1)–O(3)	2.075(7)	2.027(6)
M(1)–O(4) [*]	2.060(7)	2.027(6)
M(1)–N(1)	2.450(7)	2.368(5)
M(1)–M(1) [*]	2.2876(12)	2.4134(10)
M(1) [*] –M(1)–N(1)	177.8(2)	178.4(2)
M(1)–N(1)–N(1) [#]	176.9(2)	179.8(2)

Symmetry code: ^{*} $-x, -y + 1, -z + 1$; [#] $-x + 1, -y + 1, -z + 1$

Table S3. Crystallographic data for **1'** and **2'**

	1'	2'
empirical formula	C ₄₀ H ₂₄ F ₄ N ₂ O ₈ Ru ₂	C ₄₀ H ₂₄ F ₄ N ₂ O ₈ Rh ₂
formula weight	938.76	942.43
$\lambda / \text{\AA}$	0.799020(3)	0.799090(7)
T / K	195(1)	195(1)
Crystal system	triclinic	triclinic
Space group	<i>P</i> -1	<i>P</i> -1
$a / \text{\AA}$	9.9825(8)	9.8967(7)
$b / \text{\AA}$	10.9906(8)	10.9360(8)
$c / \text{\AA}$	11.4527(7)	11.3457(7)
$\alpha / ^\circ$	65.866(5)	65.996(5)
$\beta / ^\circ$	66.143(6)	66.173(6)
$\gamma / ^\circ$	65.088(7)	65.291(6)
$V / \text{\AA}^3$	998.2(1)	977.7(1)
$d_{\text{calcd}} / \text{g cm}^{-3}$	1.562	1.601
Z	1	1
$2\theta_{\text{max}} / ^\circ$	50.00	50.00
$2\theta_{\text{min}} / ^\circ$	3.00	3.00
R_{wp}^{a}	0.0273	0.0256
R_{B}^{b}	0.0191	0.0097
CCDC no.	895510	895508

^a $R_{\text{wp}} = [\sum w[y - f(\mathbf{x})]^2 / \sum wy^2]^{1/2}$, where y and $f(\mathbf{x})$ represent the observed intensity and the calculated intensity at a diffraction angle of 2θ , respectively. ^b $R_{\text{B}} = \sum ||F_{\text{o}}| - |F_{\text{c}}|| / \sum |F_{\text{o}}|$.

Table S4. Selected bond lengths (Å) angles (°) for **1'** and **2'** (M = Ru for **1'** and Rh for **2'**)

	1'	2'
M(1)–O(1)	2.04(7)	2.05(6)
M(1)–O(2) [*]	2.05(8)	2.05(6)
M(1)–O(3)	2.06(7)	2.02(7)
M(1)–O(4) [*]	2.05(7)	2.03(7)
M(1)–N(1)	2.50(8)	2.44(7)
M(1)–M(1) [*]	2.29(2)	2.41 (2)
M(1) [*] –M(1)–N(1)	177.3(4)	179.2(4)
M(1)–N(1)–N(1) [#]	156.3(6)	155.6(6)

Symmetry code: ^{*} $-x + 1, -y + 1, -z$. [#] $-x, -y + 1, -z$

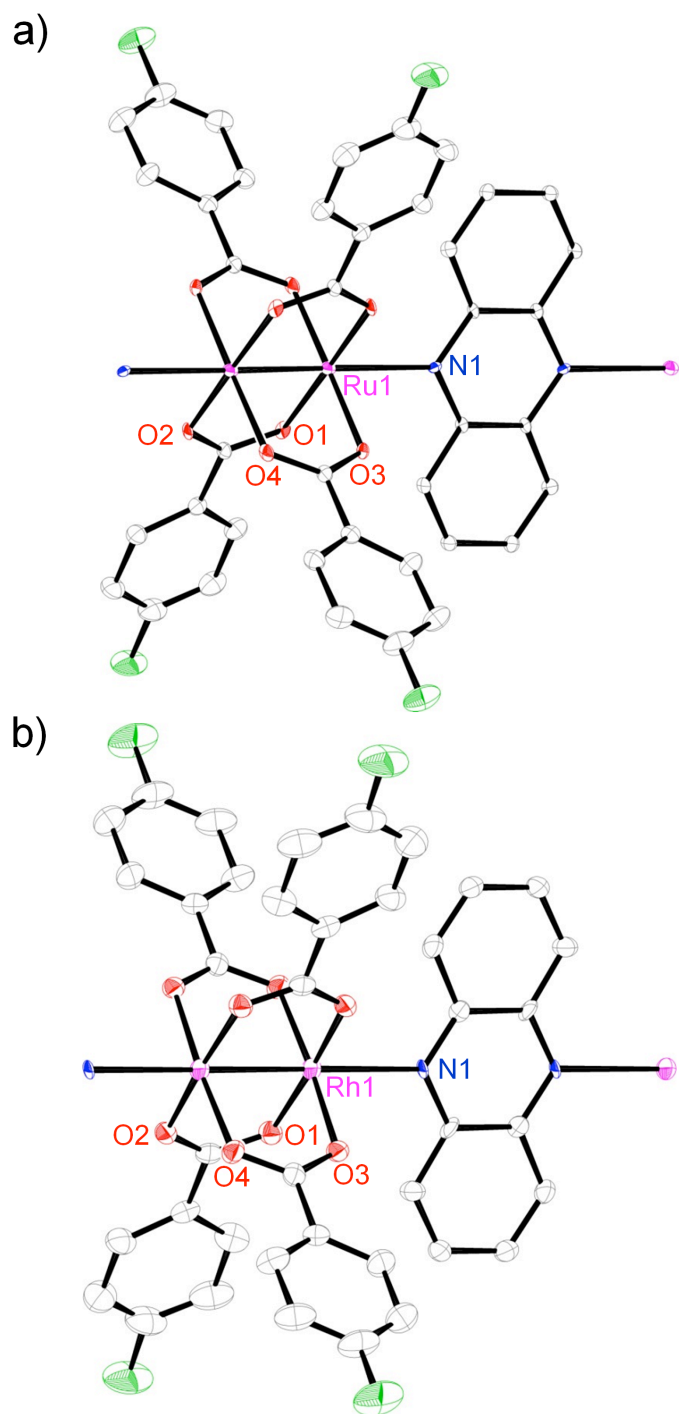


Fig. S1. Thermal ellipsoid plots of the formula unit of **1** (a) and **2** (b) with atomic numbering scheme (50% probability level). Hydrogen atoms and crystallization solvent (PhNO₂) were omitted for clarity.

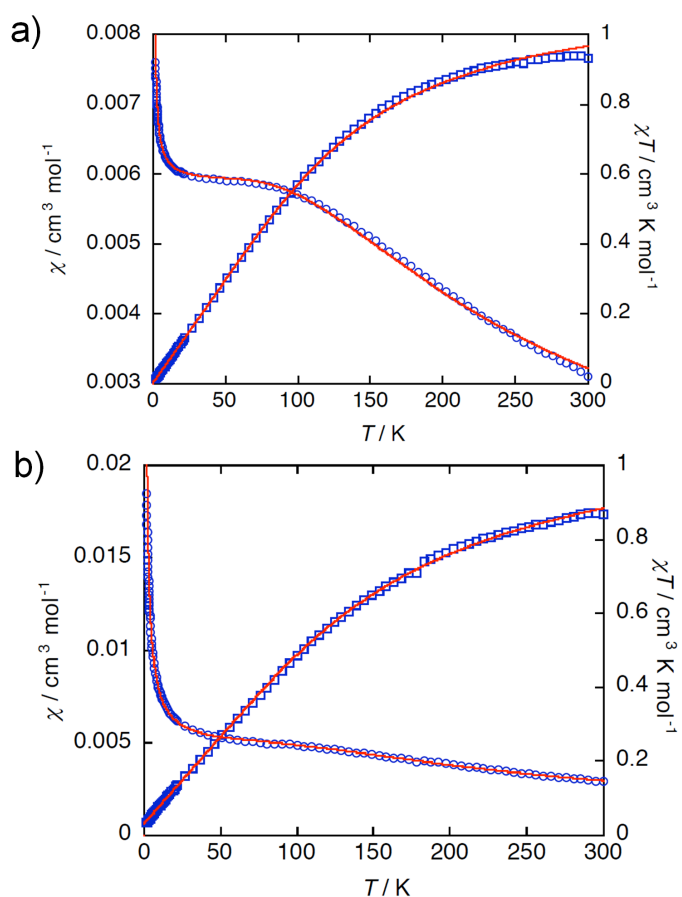


Fig. S2. Temperature dependence of χ and χT for **1** (a) and **1'** (b), where the red lines represent simulated curves based on a Curie model with $S = 1$ taking into account zero-field splitting (D), temperature-independent paramagnetism (χ_{TIP}), and impurity with $S = 3/2$ (ρ). The contribution of intermolecular interactions (zJ) was taken into account in the frame of the mean-field approximation for **1'**. The best fitting parameters were: $g = 2.0$ (fix), $D/k_{\text{B}} = 348.6(6)$ K, $\chi_{\text{TIP}} = 147(7) \times 10^{-6} \text{ cm}^3 \text{ mol}^{-1}$, and $\rho = 0.00170(1)$ for **1** and $g = 2.0$ (fix), $D/k_{\text{B}} = 353(9)$ K, $zJ/k_{\text{B}} = -29(4)$ K, $\chi_{\text{TIP}} = 198(62) \times 10^{-6} \text{ cm}^3 \text{ mol}^{-1}$, and $\rho = 0.0167(1)$ for **1'**,

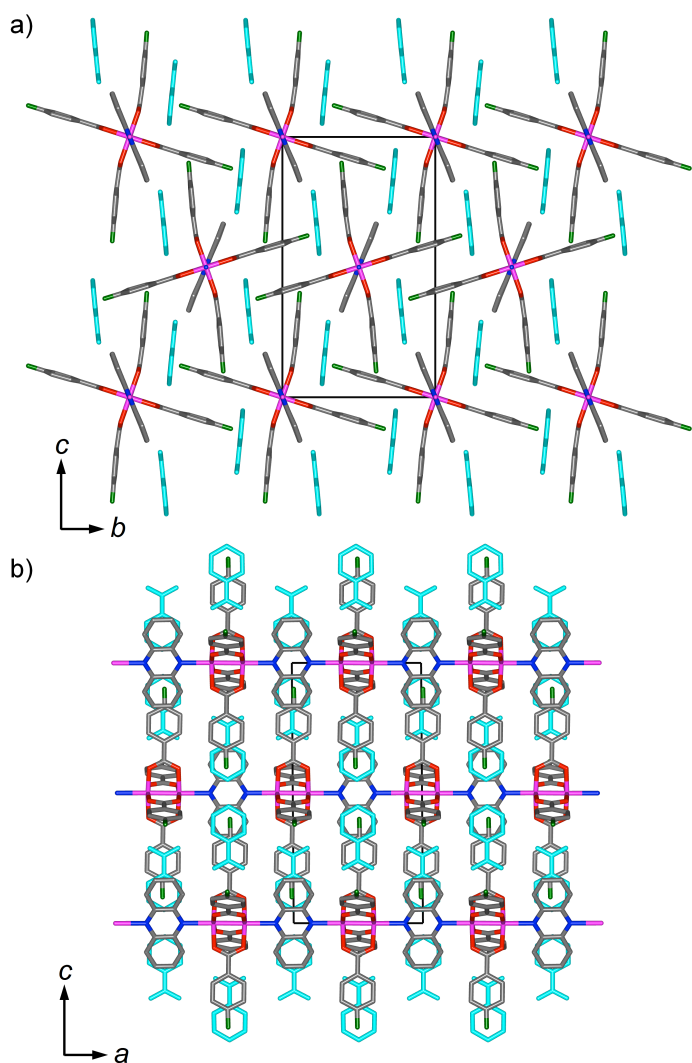


Fig. S3. Packing view of **2**, where blue, red, gray, green and purple represent N, O, C, F and Rh, respectively, PhNO₂ molecules are represented in cyan, and hydrogen atoms are omitted for clarity. (a) The projection to the *bc* plane (i.e., along the chain direction). (b) The projection to the *ac* plane.

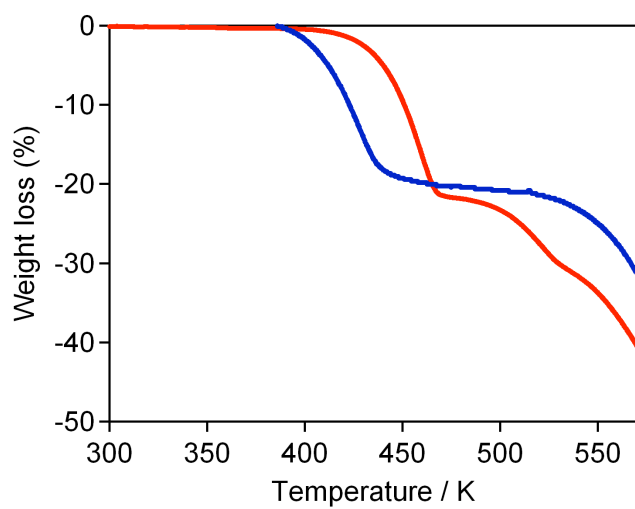


Fig. S4. TGA profiles of **1** (red) and **2** (blue) with a heating rate of $5 \text{ K} \cdot \text{min}^{-1}$.

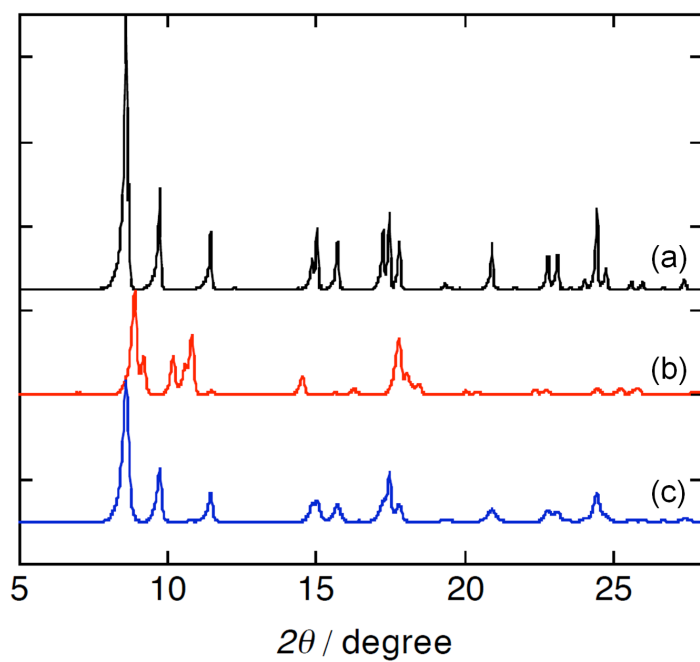


Fig. S5. XRPD patterns of **1** as synthesized (a), **1'** obtained by drying **1** *in vacuo* at 400 K for 5 h (b), and the material obtained by exposing **1'** to a PhNO₂ vapor at 298 K for 72 h (c). Data obtained using Cu $K\alpha$ radiation ($\lambda = 1.54 \text{ \AA}$).

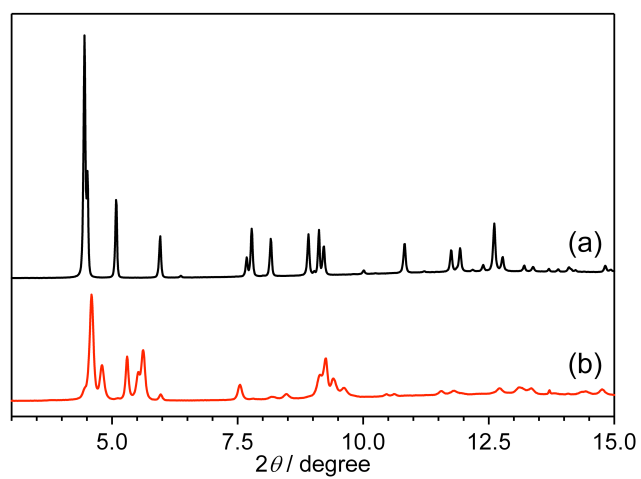


Fig. S6. XRPD patterns of **2** as synthesized (a) and **2'** obtained by drying **2** *in vacuo* at 400 K for 5 h (b). Data obtained using synchrotron radiation ($\lambda = 0.80 \text{ \AA}$).

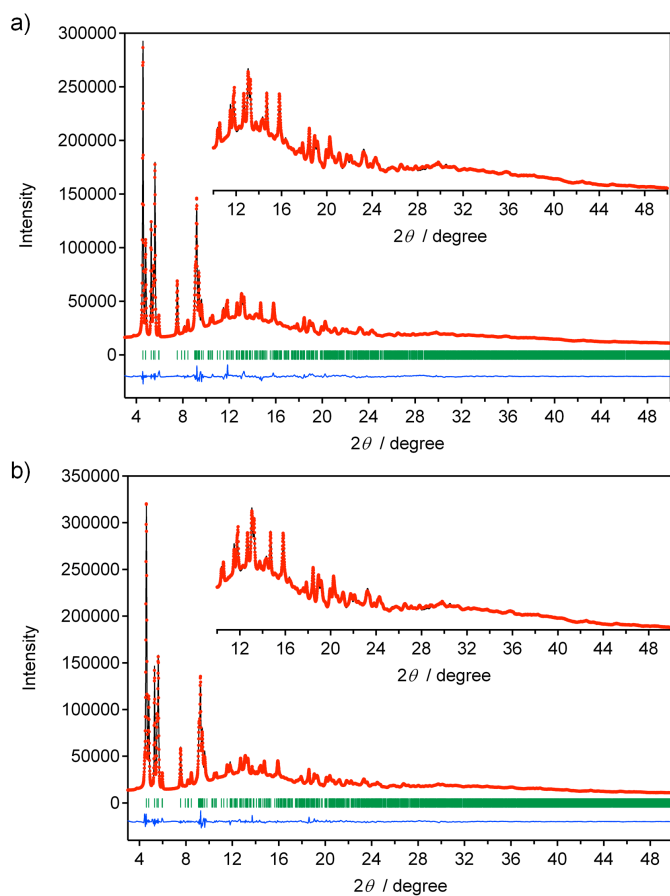


Fig. S7. XRPD pattern at 195 K and Rietveld analysis for **1'** (a) and **2'** (b). Red dots, black line, and blue line are the observed plots, calculated pattern, and their difference, respectively. Green bars represent the calculated positions of the Bragg reflections.

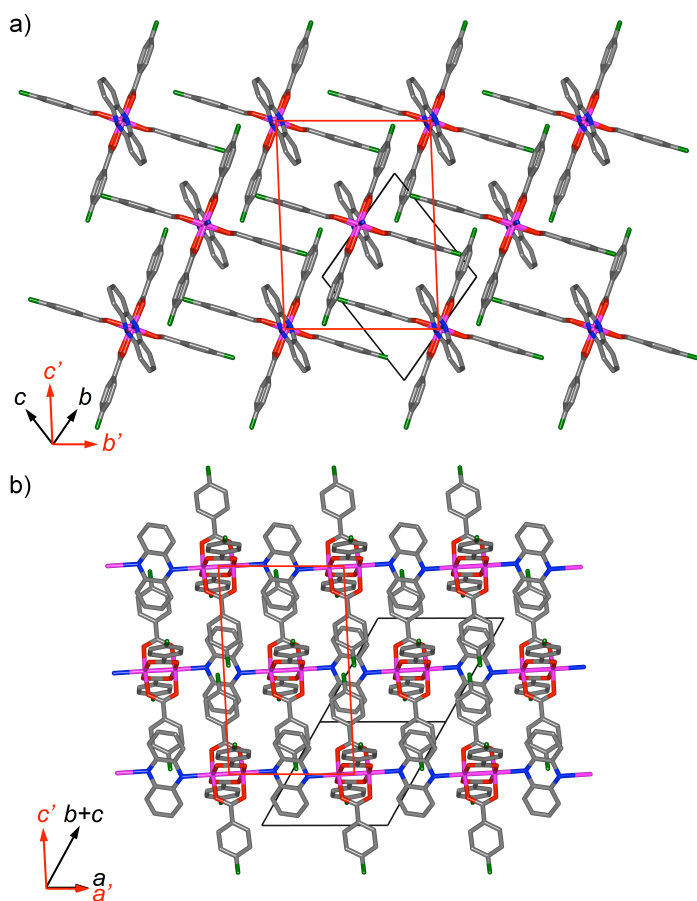


Fig. S8. Packing views of **2'**, where blue, red, gray, green and purple represent N, O, C, F and Rh, respectively, and hydrogen atoms are omitted for clarity. (a) The projection to the *bc* plane. (b) The projection along the $[01\bar{1}]$ direction. The unit cell in red represents a composite lattice for an easy comparison with the lattice of solvated phase (see text). The unit cell parameters for **2'** was transformed into: $a' = 9.8967(7) \text{ \AA}$, $b' = 12.1397(11) \text{ \AA}$, $c' = 16.3098(11) \text{ \AA}$, $\alpha' = 92.608(9)^\circ$, $\beta' = 92.507(7)^\circ$, $\gamma' = 90.057(6)^\circ$, $V' = 1955.4(2) \text{ \AA}^3$, $Z = 2$, where $a' = a$, $b' = b - c$, $c' = -a + b + c$.

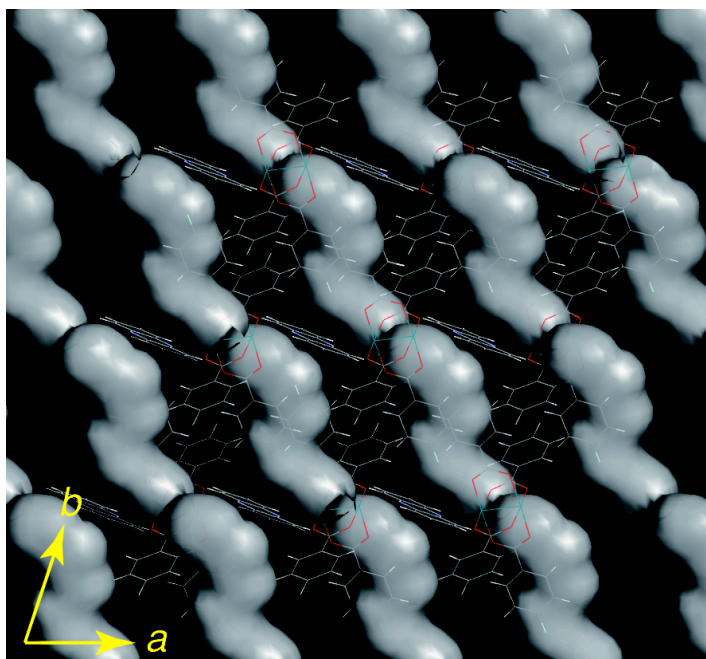


Fig. S9. Connolly surfaces of 1D channels in **2'** as the projection to the *ab* plane, which run along the $[-110]$ direction.

References for ESI

- 1 H. Miyasaka, N. Motokawa, R. Atsuumi, H. Kamo, Y. Asai, M. Yamashita, *Dalton Trans.*, 2011, **40**, 673.
- 2 R. S. Drago, S. Peter Tanner, R. M. Richman, J. R. Long, *J. Am. Chem. Soc.*, 1979, **101**, 2897.
- 3 E. A. Boudreaux, L. N. Mulay, *Theory and Applications of Molecular Paramagnetism*, Eds. John Wiley & Sons, New-York, 1976.
- 4 M. C. Burla, R. Caliandro, M. Camalli, B. Carrozzini, G. L. Cascarano, L. De Caro, C. Giacovazzo, G. Polidori, D. Siliqi, R. Spagna, *J. Appl. Cryst.*, 2007, **40**, 609.
- 5 G. M. Sheldrick, *Acta Cryst. A*, 2008, **64**, 112.
- 6 K. Momma, F. Izumi, *J. Appl. Cryst.*, 2008, **41**, 653.
- 7 A. L. Spek, *Acta Cryst., Sec. A*, 1990, **46**, 194.
- 8 V. Favre-Nicolin, R. Černý, *J. Appl. Cryst.*, 2002, **35**, 734.
- 9 F. Izumi, K. Momma, *Solid State Phenom.*, 2007, **130**, 15.
- 10 F. A. Cotton and R. A. Walton, *Multiple Bonds Between Metal Atoms*, 2nd ed., Oxford University Press, Oxford, 1993.
- 11 H. Miyasaka, N. Motokawa, T. Chiyo, M. Takemura, M. Yamashita, H. Sagayama and T. Arima, *J. Am. Chem. Soc.*, 2011, **133**, 5338.